Table of Content

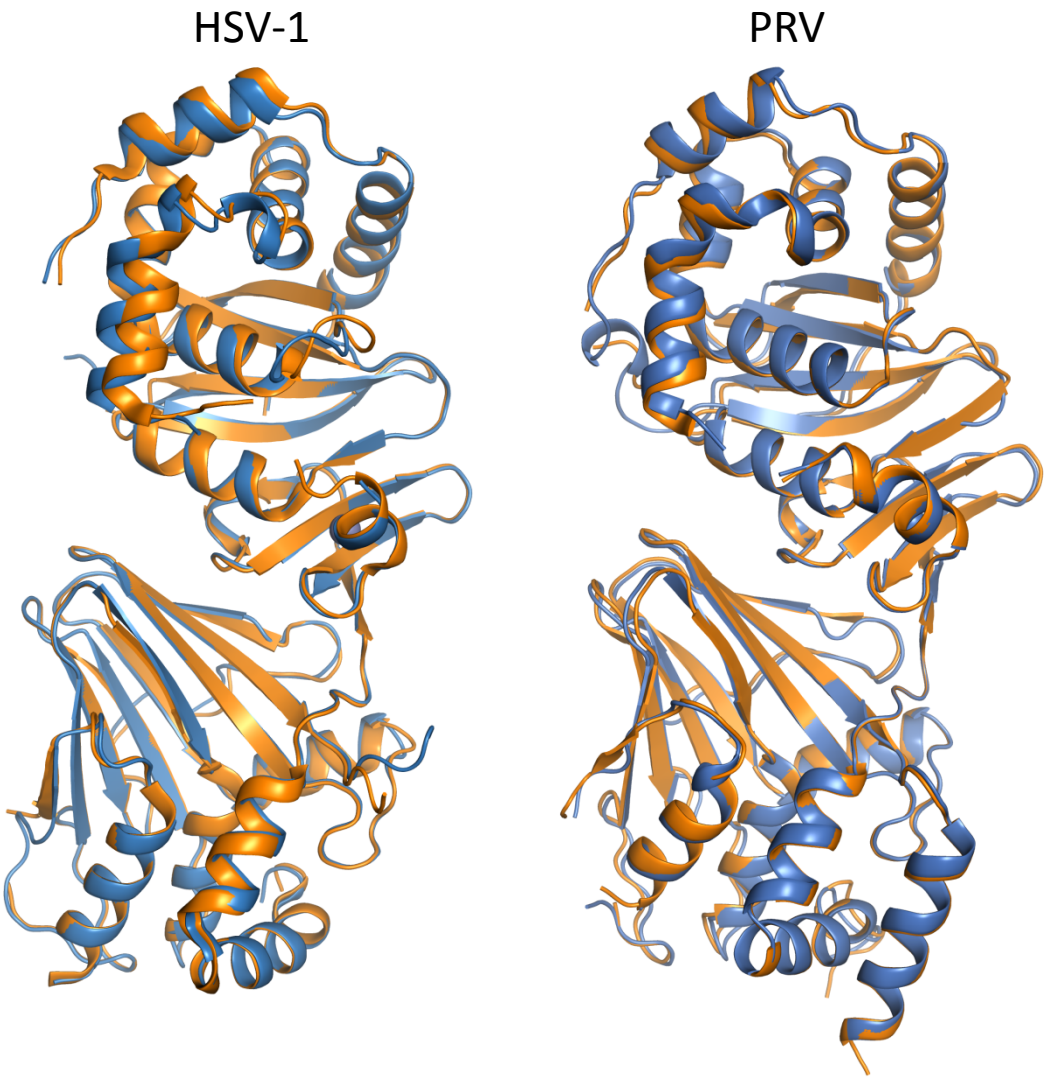

Figure S1: Superposition of NCS mates in for HSV-1 and PRV NEC. Chains A and B are in orange, chains C and D in dark blue. HSV-1 NECs superpose with an RMSD of 0.42 Å and PRV NECs with an RMSD of 0.60 Å.

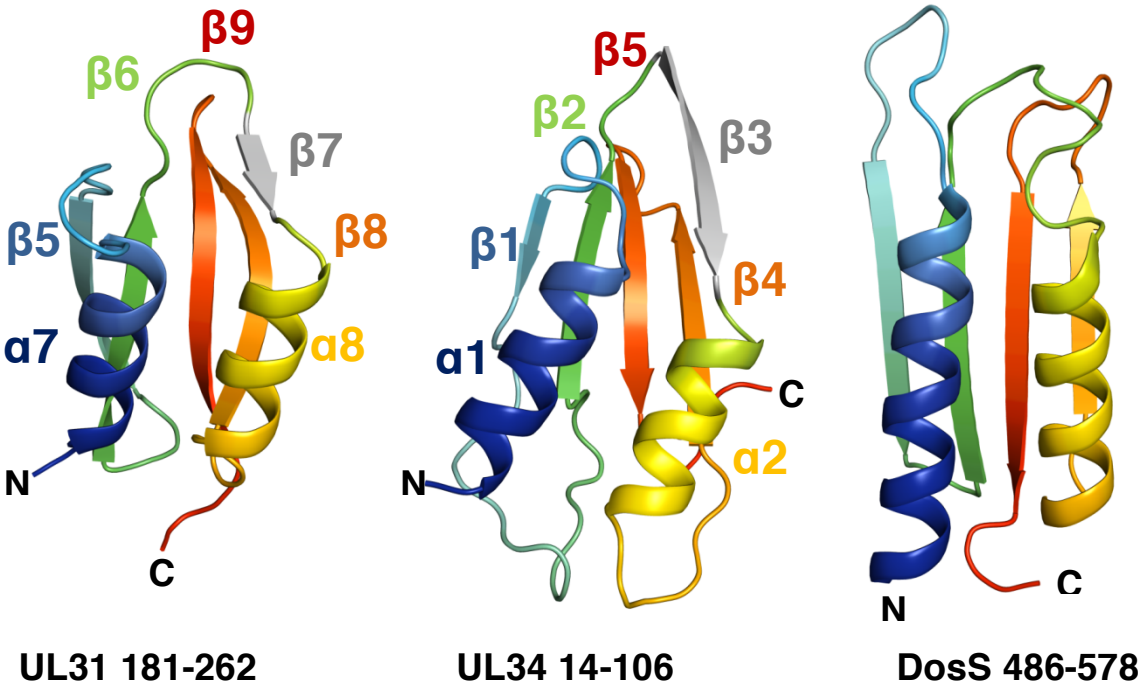

Figure S2: Comparison of HSV-1 UL31 and UL34 Bergerat-like fold to DosS ATP-binding domain. The molecules are colored in rainbow ranging from blue (N terminus) to red (C terminus). The additional β strand, which is not present in DosS or other members of the GHKL ATPase/kinase superfamily, is colored in grey. UL31 181-262 and UL34 14-106 overlay with an rmsd of 4.28 Å. The Bergerat fold in DosS (486-578) superposes onto UL31 with a Z-score of 3.9 and an RMSD of 3.99 Å and onto UL34 with a Z score of 3.4 and an RMSD of 5.28 Å. Neither UL31 nor UL34 contain a nucleotide-binding pocket.

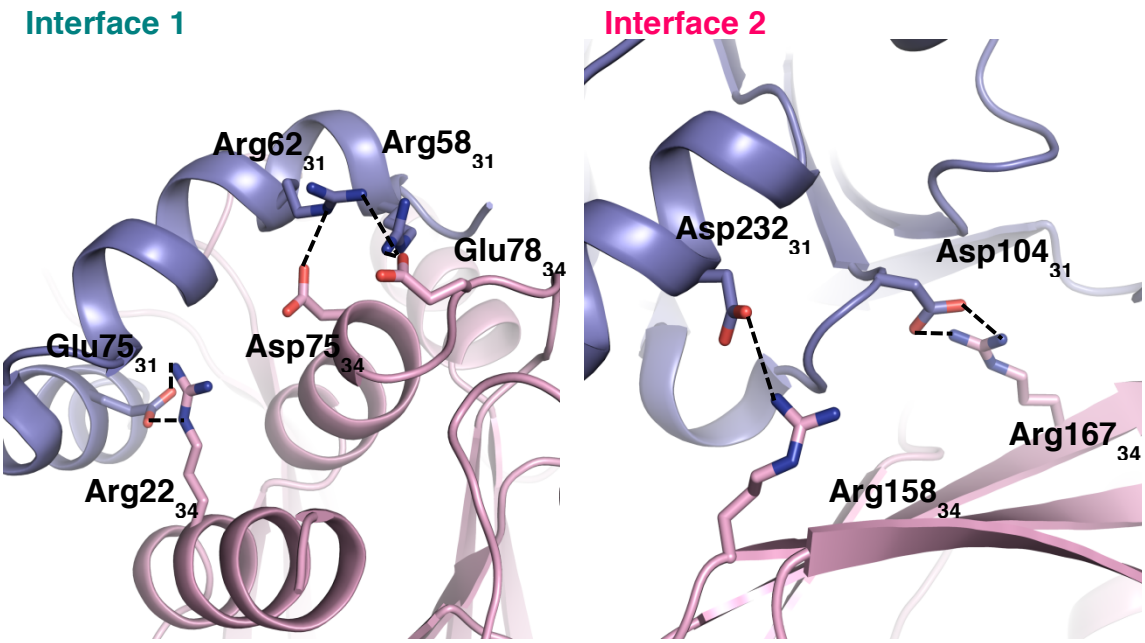

Figure S3: Salt bridges at interface 1 and 2 in HSV-1 NEC. UL31 is colored slate and UL34 pink.

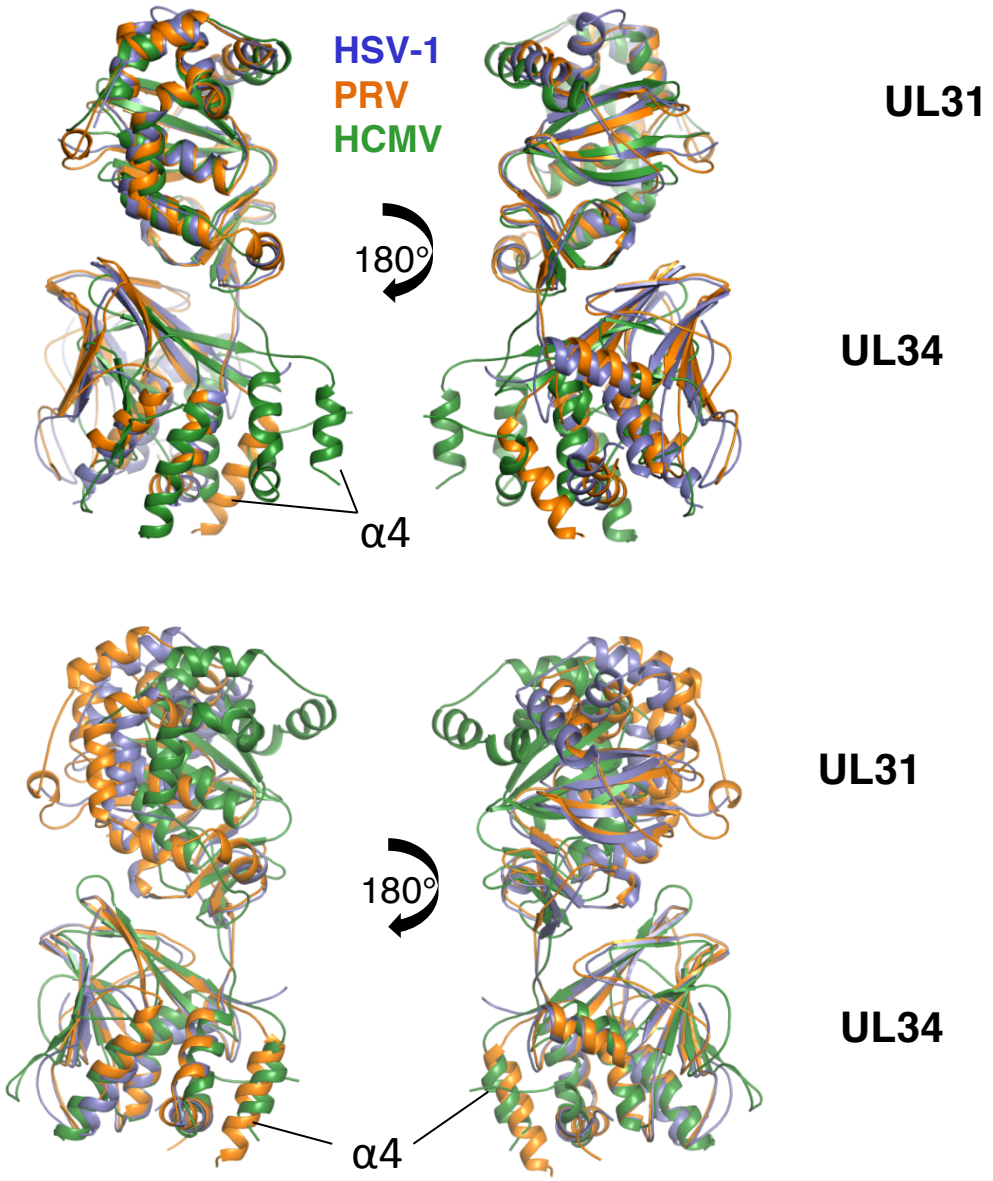

Figure S4: Superposition of NEC from HSV-1, PRV and HCMV. HSV-1 NEC is shown in slate, PRV NEC in orange and HCMV NEC in forest. While the individual NEC subunits, UL31 and UL34, are very similar in all three complexes, their relative orientations vary, especially between the NECs from α- and β-herpesviruses. In the top panel, PRV UL31 and HCMV UL53 were superposed onto HSV-1 UL31 to show differences in UL34 (or HCMV UL50) orientations. Compared to HSV-1 UL34, PRV UL34 is shifted to the left (left panel), whereas HCMV UL50 is shifted to the right. Note that helix α4, while present in both PRV UL34 and HCMV UL50, is positioned differently, strengthening the hypothesis that this helix is flexible. The RMSD between HSV-1 UL31 and HCMV UL53 is 2.10 Å. All loops are smoothened for clarity. In the bottom panel, PRV UL34 and HCMV UL50 were superposed onto HSV-1 UL34. The RMSD between HSV-1 UL34 and HCMV UL50 is 1.63 Å.

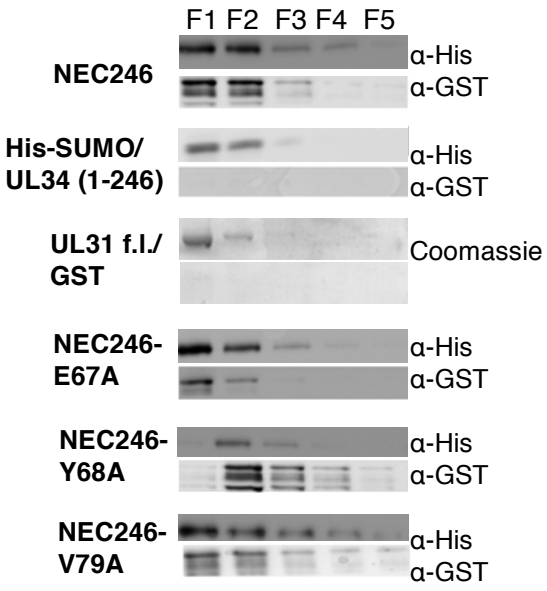

Figure S5: *In vitro* NEC formation of UL31 and UL34 mutants. Constructs were coexpressed in *E. coli* and purified using Ni-NTA affinity chromatography. The first five fractions (F1-F5) after extensive washing are shown. His-SUMO-UL31 and GST-UL34 were detected by 12% SDS-PAGE and analyzed either by Coomassie staining or by Western Blot with anti-His or anti-GST antibodies, respectively. NEC246 contains His-SUMO-UL31 and GST-UL34(1-246) and serves as a positive control. For negative controls, UL31 or UL34 were coexpressed with GST or His-SUMO, respectively. No complex formation was observed for the negative controls, but all mutants were able to form complexes. GST-UL34(1-246) is prone to degradation.

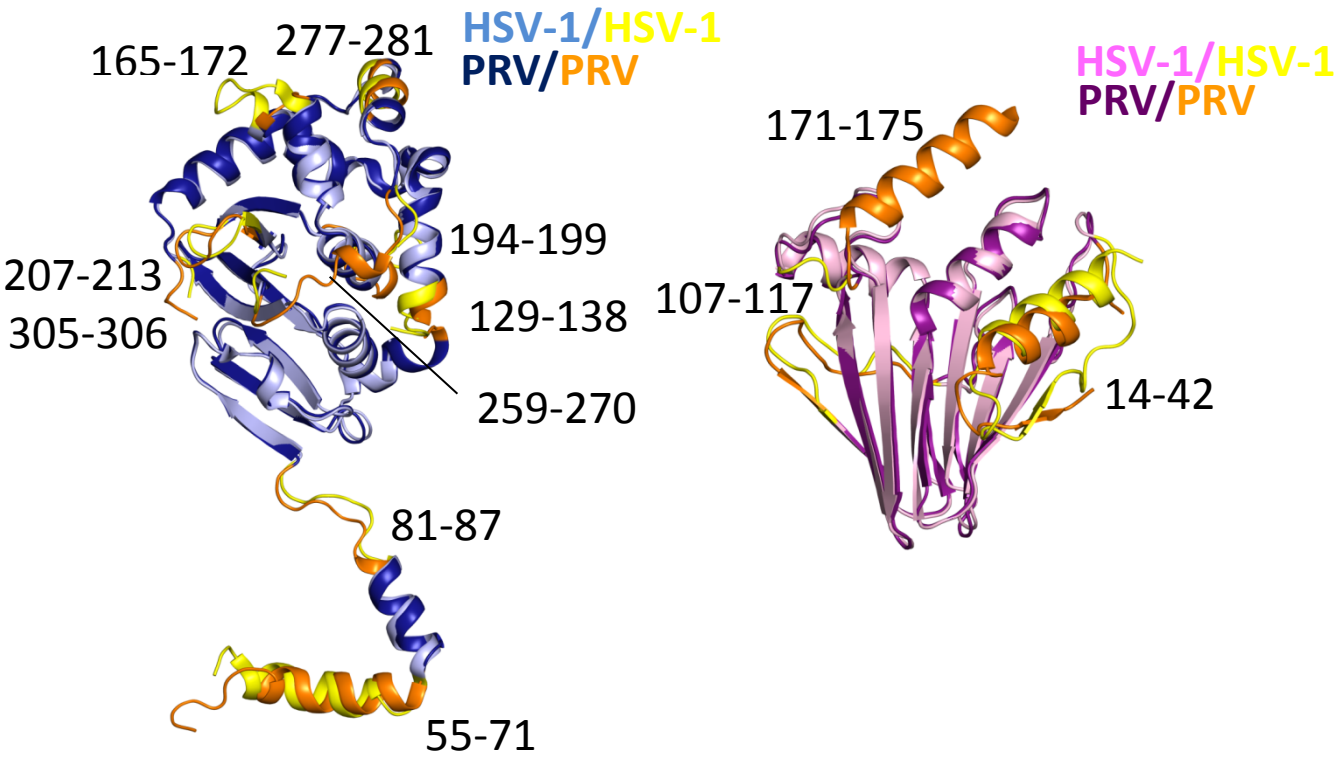

Figure S6: Superposition of HSV-1 and PRV UL31 and UL34. HSV-1 UL31 is shown in lightblue and UL34 in lightpink. PRV UL31 is shown in blue and UL34 in purple. Regions with variation are labeled with the residues in HSV-1 and coloured yellow or orange for HSV-1 and PRV, respectively. The rmsd for UL31 is 1.169 Å and for UL34 0.690 Å. The main difference is helix α4 in UL34, which is not resolved in the HSV-1 structure.

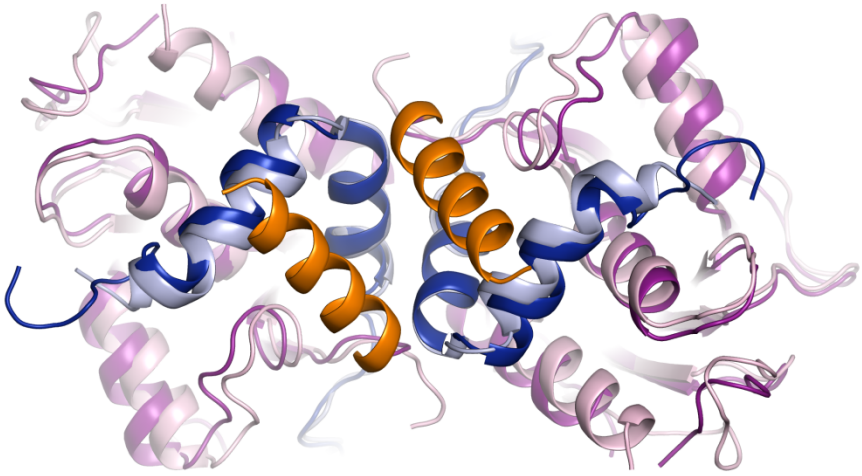

Figure S7: Superposition of HSV-1 and PRV NEC within the hexagonal lattice. UL31 is colored lightblue in HSV-1 and darkblue in PRV. UL34 is colored lightpink in HSV-1 and purple in PRV. Helix α4 is colored orange. Dimer-formation and thus hexagonal lattice formation in HSV-1 would not be possible with α4 in this position.

Table S1: Residues involved in HSVi 1 NEC formation. Conserved residues in αi herpesviruses are in bold, strictly conserved residues in αi , βi and γi herpesviruses are bold and underlined. Residues involved in salt bridges and hydrogen bonds are not repeated in Hi bond column. Residues are from chains C and D.

	Interface 1				**Interface 2**			
	Salt bridge	*H-bond*	*hydrophobic*		*Salt bridge*	*H-bond*	*hydrophobic*	
HSV-1 UL31	**Arg58**	**His56**	**Leu55**	**Val79**	**Asp104**	Gln100	Val87	Thr236
	Arg62	Arg60	Glu57	**Leu82**	**Asp232**	**Ala103**	Thr90	Pro239
	Glu75	**Tyr61**	Leu64	**Pro85**		**Asn105**	Pro91	
		Phe65	Ala66				Asp99	
		Arg80	Leu68				Thr101	
		Ser81	Ala69				**Val102**	
		Ser83	**Pro72**				Leu116	
		Val84	Ile76				Ile118	
		Leu86	Ile78				Leu135	
HSV-1 UL34	**Arg22**	Ile26	Leu25	Gly131	**Arg158**	**Asn117**	Glu114	
	Asp75	**Tyr68**	Val27	Asp134	**Arg167**	**Gln163**	Arg115	
	Glu78	**Arg71**	Pro28	Leu142			Thr116	
		Asn74	Ser29	**Asp143**			Val118	
		Lys137	**Pro65**	**Arg145**			Ile119	
		Ala144	**Glu67**	**Pro146**			**Phe156**	
		Met147	Leu72	Met148			Arg161	
		Phe168	**Ala77**	Ala149			**Leu164**	
		Gly170	Pro80	Ser150			Ala165	
		Glu172	**Cys81**	Trp152				
			Asn82	Met169				
			Pro83	**Pro171**				
			Leu130	Gly175				

Table S2: Residues involved in PRV NEC formation. Conserved residues in αi herpesviruses are in bold, strictly conserved residues in α-, β- and γ-herpesviruses are bold and underlined. Residues involved in salt bridges and hydrogen bonds are not repeated in H-bond column. Residues are from chains A and B.

	Interface 1				**Interface 2**			
	Salt bridge	*H-bond*	*hydrophobic*		*Salt bridge*	*H-bond*	*hydrophobic*	
PRV UL31	**Glu42**	**Arg 25**	Thr19	**Ala37**	**Asp71**	Pro58	Ile54	Lys22
		Tyr28	Ala23	**Pro39**	**Asp195**	Gln67	Ala57	
		Tyr31	Ala24	Asp41		**Ala70**	Val59	
		Tyr34	Arg27	Val43		**Asn72**	Gly66	
		Gln38	Ala29	Thr44			Ala68	
		Arg47	Pro30	Thr45			Val69	
		Gly48	Phe32	**Val46**			Leu83	
		Ser50	Ala33	**Leu49**			Leu85	
		Asn51	Ala35	**Pro52**			Leu198	
		Leu53	Ala36				Ala202	
PRV UL34	**Arg8**	Ser14	Leu11	**Arg131**	**Arg144**	His101	Ala99	
		Tyr54	Ile12	**Pro132**	**Arg153**	**Asn103**	Glu100	
		Ala63	Gly15	Arg134		**Gln149**	Ile105	
		Leu133	Asn47	Ala135			Phe142	
		Phe154	**Pro51**	Met136			**Pro146**	
		Gly156	**Arg57**	Met155			Arg147	
		Asp158	Leu58	**Pro157**			**Leu150**	
		Arg169	Arg60	Gln162			Ser151	
		Arg173	Ser61	Thr163			**Phe154**	
			His64	Leu166				
			Pro66	Leu167				
			Asp120	Ala170				
			Val128	Glu171				
			Asp129	Gln174				
			Thr130					

Table S3: Residues involved in hexameric lattice formation. Conserved residues in αi herpesviruses are in bold, strictly conserved residues in αi , βi and γi herpesviruses are bold and underlined.

	UL31 (D)	**UL34 (C)**	**Interface area (Å^2)**
Hexamer	86, 87, 88, 89, 91, 92, 93, **94**, **<u>110</u>**, **111**, **112**, **113**, **114**, 222, **246**, **247**, **248**, 249, 250, **252**, 260, 262, 301, 302	37, 40, 41, 45, 46, **47**, 48, 49, **53**, 55, 57, 88, **90**, **<u>91</u>**, **92**, **93**, **95**, 101, 102, **103**, 104, 113, 114, 122, **123**, 138, 139, 140, **141**, 142, **143**, 159, **160**, 161, 175	864
Dimer 1	**72**, 73, 74, 76, 77, 78, 80, 81, 83, **120**, 126, 127, 136, 138, 139, 141, 142, 145, 146, 229, **269**	21, 25, 29, 32, 59, **171**, 172, 173, 174	697
Trimer	149, 150, 152, 153, **155**, **286**, **287**, 288, **291**, 295		180
	UL31 (B)	**UL34 (A)**	
Hexamer	86, 87, 88, 89, 93, **94**, **<u>110</u>**, **111**, **112**, **113**, **114**, 115, 222, **246**, **247**, **248**, 249, 250, 251, **252**, 260, 302	32, 33, 37, 40, 41, 45, 46, **47**, 48, 49, **53**, 54, 55, 57, 58, 88, **90**, **<u>91</u>**, **92**, **93**, **95**, **103**, 104, 112, 113, 114, 122, **123**, 138, 139, 140, **141**, 142, 159, **160**	841
Dimer 1	**72**, 73, 76	14, 17, 18, 21, 22, 25, 29, 30, 32	286
Dimer 2	**286**, **287**, 288, **291**, 295		106
Trimer	136, 138, 139, 141, 142, 145, 146, 149, 150, 152, 153, **155**, 193, 195, 196, 197, **269**		237

Table S4: Previously described noni functional mutants in HSVi 1 and PRV. SB: salt bridge, HB: hydrogen bond. In double or triple mutants only underlined residue is focused on.

Solvent-inaccessible/NEC interface						
Residue in HSV-1	**Mutation**	**Virus tested**	**Phenotype**	**Location in structure**	**In vicinity of/interaction with**	**Reference**
UL34 Δ1-23	deletion	PRV, HCMV	No NEC formation	α1	$E75_{31}$(SB), $F65_{31}$(HB)	Passvogel et al., 2013; Milbradt et al., 2012
UL34 D58/D61/E62	A/A/A	HSV-1	Reduced complementation	β2- β3	$R158_{34}$(SB)	Bjerke et al., 2003
UL34 E67	A	HSV-1/PRV	No NEC formation	α2	$K137_{34}$(SB)	Bjerke et al., 2003; Bubeck et al., 2004; Passvogel et al., 2013
UL34 Y68	A	HSV-1/PRV	No NEC formation	α2	$E75_{31}$(HB), $I26_{34}$, $P65_{34}$, $V79_{31}$	Bubeck et al. 2004; Passvogel et al., 2013
UL34 E67/V69	A/A	HSV-1	Not at INM	α2	$I23_{34}$, $K137_{34}$(SB), $L130_{34}$	Bjerke et al., 2003
UL34 L70	A	PRV	Reduced complementation	α2	$P83_{34}$, $L85_{34}$, $M73_{34}$, $N74_{34}$	Paßvogel et al., 2014
UL34 C81	A	PRV	Decreased plaque size	α2-β4	$H101_{34}$, $L46_{34}$	Paßvogel et al., 2013
UL34 N89	A	PRV	No NEC formation	β4	$G91_{34}$(HB), $P160_{34}$(HB), $L120_{34}$(HB)	Paßvogel et al., 2014
UL34 G91	A	PRV	No NEC formation	β4-β5	$S122_{34}$	Paßvogel et al., 2014
UL34 N117	A	PRV	No complementation	β6	$N105_{31}$(HB)	Paßvogel et al., 2014
UL34 L120	A	PRV	No NEC formation	β6	$E124_{34}$-$T126_{34}$	Paßvogel et al., 2014
UL34 L130	A	PRV	No NEC formation	α3	$L70_{34}$, $R71_{34}$, $H56_{31}$	Paßvogel et al., 2014
UL34 K137/R139	A/A	HSV-1	No complementation	α3	$E67_{34}$(SB), $Y61_{31}$(SB)	Bjerke et al., 2003
UL34 C155	A	PRV	Decreased plaque size	β8	$V94_{34}$	Paßvogel et al., 2013
UL34 R158/R161	A/A	HSV-1	No complementation	β8- β9	$D61_{34}$(SB), $D232_{31}$(SB)	Bjerke et al., 2003
Solvent-accessible						
Residue in HSV-1	**Mutation**	**Virus tested**	**Phenotype**	**Location in structure**	**Oligomeric interface**	**Reference**
UL34 D35/E37	A/A	HSV-1	No budding	β1- β2	hexamer	Roller et al., 2010
UL34 D58/D61/E62	A/A/A	HSV-1	Reduced complementation	β2- β3	hexamer	Bjerke et al., 2003
UL34 K137/R139	A/A	HSV-1	No complementation	α3	hexamer	Bjerke et al., 2003
UL34 R158/R161	A/A	HSV-1	No complementation	β9	hexamer	Bjerke et al., 2003
UL31 L291	A	PRV	Budding impaired	α10	No (capsids binding site?)	Paßvogel et al., 2015

Table S5: Average ratios of ILV containing GUVs divided by the total number of GUVs counted. For each set of mutants a negative (no protein) and positive control (wild type) were counted as they vary with each experiment. These values are indicated at the top of each set. To obtain the percentages shown in figure 6C, the background was subtracted from wildtype and mutant values. Mutant values were then divided by wildtype and multiplied by 100%.

Mutant	**AVG (ILV-GUVs)/(total GUVs)**
Set 1 (wildtype: 0.117, background: 0.006)	
V92F	0.024
G91R	0.138
D286R	0.086
E153R	0.058
F252Y	0.051
DN	0.017
DN/SUP	0.116
Set 2 (wildtype: 0.118, background: 0.009)	
T123Q	0.046
Set 3 (wildtype: 0.187, background:0.096)	
E37A	0.081
Set 4 (wildtype: 0.208, background:0.095)	
V247F	0.128
SUP	0.250
L142E	0.157
R49A	0.180
Set 5 (wildtype: 0.070, background: 0.007)	
V92F/SUP	0.072